Supplementary Materials

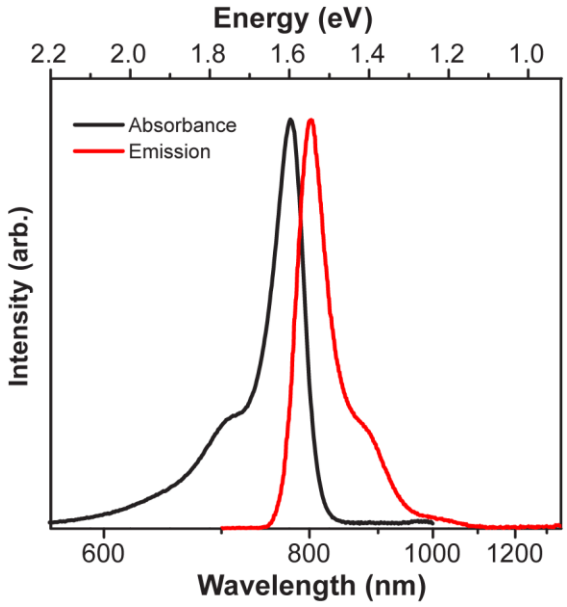

Supplementary Figure 1. Optical properties of IRDye 800 CW PEG. The absorption spectrum (black) of aqueous IRDye 800CW exhibits a peak at 776 nm, with a higher energy shoulder extending into visible wavelengths. The emission spectrum (red) of aqueous IRDye 800CW mirrors the absorption spectrum, exhibiting an emission peak at 801 nm and a lower energy shoulder extending into SWIR wavelengths.

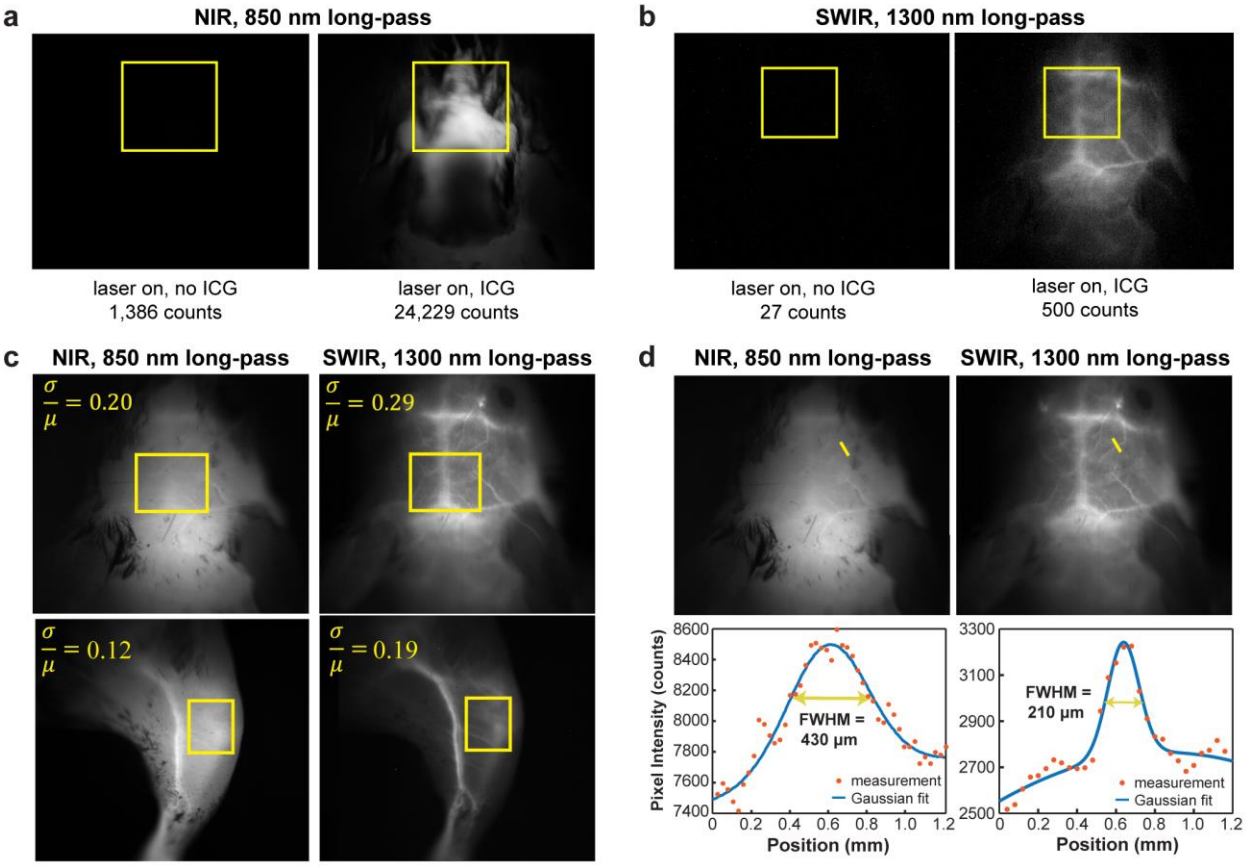

Supplementary Figure 2. Control images and contrast quantification of brain and hind limb vasculature in a mouse. Aqueous ICG was injected into the tail vein of two mice. (a) The first mouse was imaged before and after ICG injection with 850 nm longpass NIR detection. Comparing the two images we see that the scattering of ICG signal is caused by the tissue, and the poor contrast is not attributed to leak-through of 808 nm excitation light being imaged on the NIR camera. (b) Similarly, there is minimal leak-through of excitation light imaged on the SWIR camera, and the majority of detectable signal comes from ICG after being injected. (c) The contrast, defined as the standard deviation (σ) divided by the mean (μ) pixel intensity, was quantified to compare NIR and SWIR imaging of the brain vasculature and hind limb vasculature of a mouse. The contrast was found to be 0.20 for NIR-imaged brain vasculature and 0.29 for SWIR-imaged brain vasculature. The contrast was 0.12 and 0.19 for NIR- and SWIR-imaged hind limb vasculature respectively. (d) Apparent vessel width was also calculated by finding the full width at half maximum of a two-term Gaussian fit to the intensity profile of a brain vessel. The apparent vessel width was 430 μm and 210 μm for NIR- and SWIR-imaged brain vasculature, respectively.

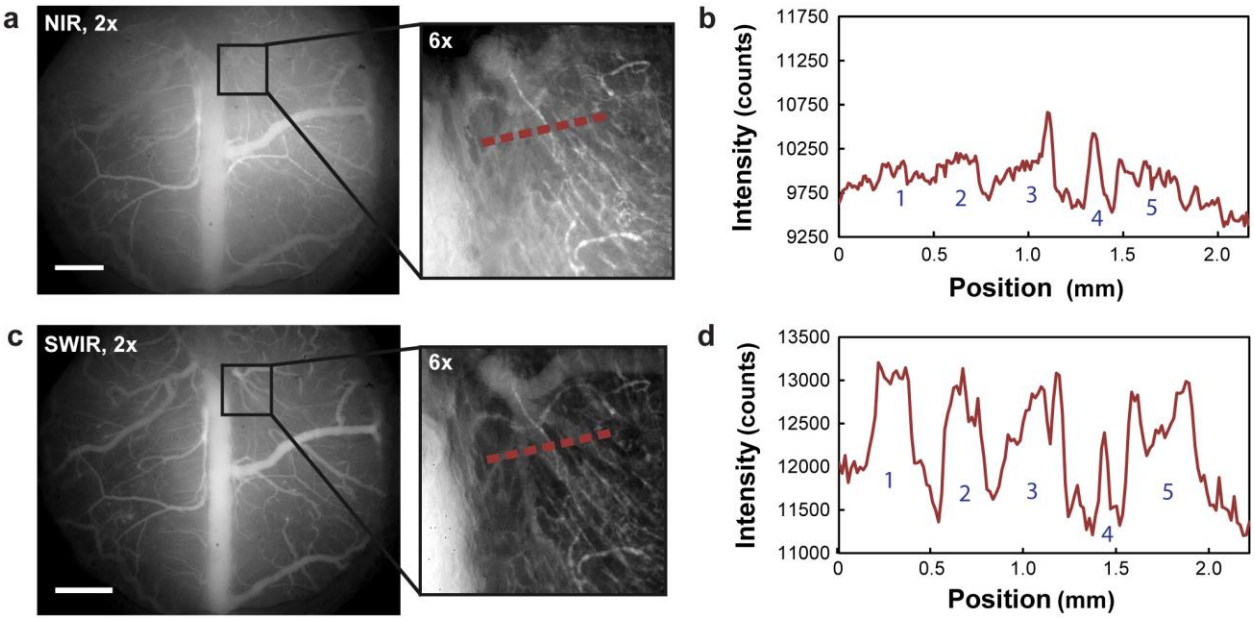

Supplementary Figure 3. High contrast SWIR microscopy of mouse brain vasculature. (a) Microscopy of brain vasculature through a cranial window in a mouse shows poor contrast with 850 nm longpass NIR detection. (b) The intensity across a line of interest shows insufficient contrast to resolve overlapping vessels from background signal. (c) Using 1300 nm longpass SWIR detection greatly improves image contrast and (d) resolution of vessels.

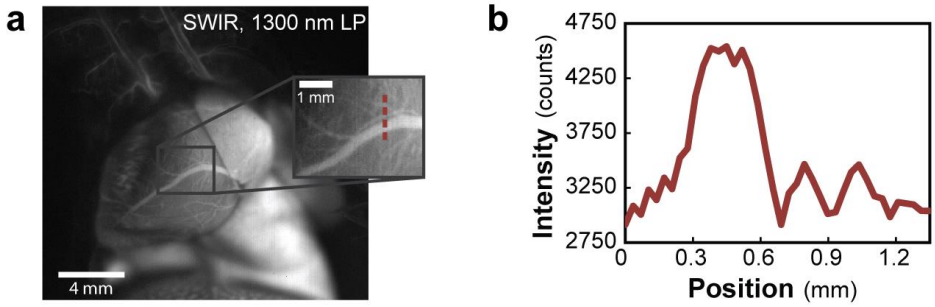

Supplementary Figure 4. Temporal and spatial resolution in ICG angiography. SWIR fluorescence angiography was performed in a mouse heart at 9.17 frames per second using ICG for contrast, diffuse 808 nm excitation, and a 1300 nm longpass emission filter on an InGaAs SWIR camera. (a,b) High spatial resolution was demonstrated by measuring fine vasculature on the order of 100 μm in diameter.

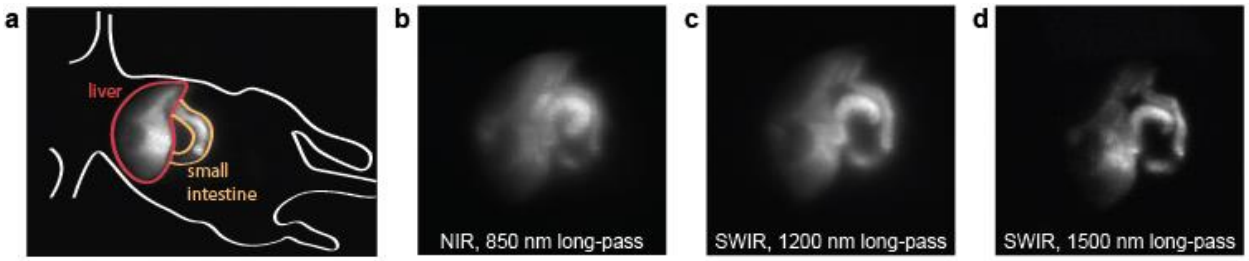

Supplementary Figure 5. Hepatobiliary clearance of ICG imaged in the SWIR beyond 1500 nm. (a) ICG contrast was used to noninvasively image the liver and small intestine in a mouse, outlined here in red and yellow respectively. (b) The liver and small intestine imaged in the NIR on a silicon camera with an 850 nm longpass filter is shown. (c) The liver and small intestine were also able to be imaged in the SWIR on an InGaAs camera with a 1200 nm longpass filter and (d) a 1500 nm longpass filter.

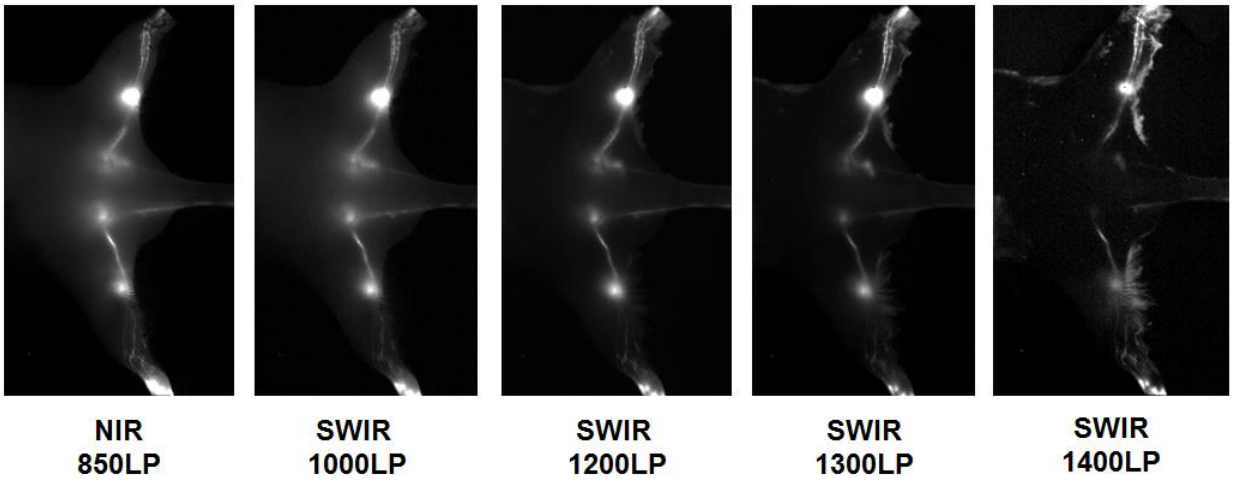

Supplementary Figure 6. Lymph node tagging with ICG SWIR fluorescence. ICG was injected subcutaneously into the footpads and tail of a mouse, excited with 50-70 mW/cm^2 of 808 nm excitation light, and imaged noninvasively through the skin as it localized in lymphatic vasculature and nodes. The lymphatic system was imaged in the NIR with an 850 nm longpass filter on a silicon camera and in the SWIR with 1000 nm, 1200 nm, 1300 nm, and 1400 nm longpass filters on an InGaAs camera. While image contrast improves at longer wavelengths, deep lymph node signal is attenuated.

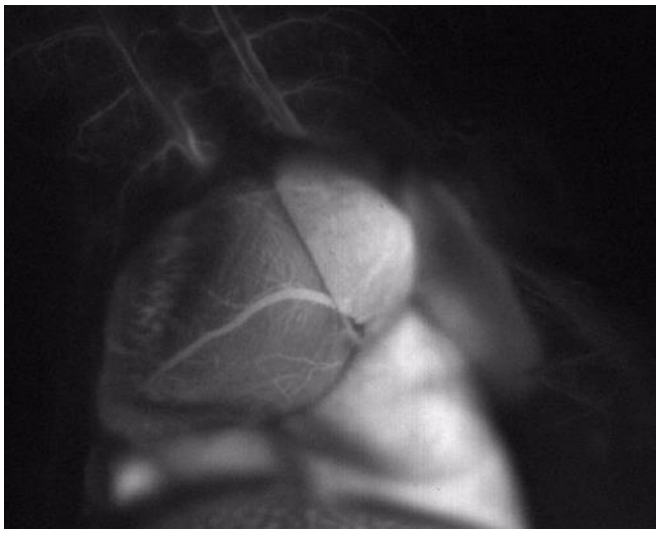

Supplementary Video 1. ICG SWIR angiography in a mouse heart. ICG fluorescence was imaged at wavelengths between 1300 nm and 1620 nm on an InGaAs SWIR camera, acquiring at 9.17 fps to image the fine vasculature on the surface of the heart while in motion.

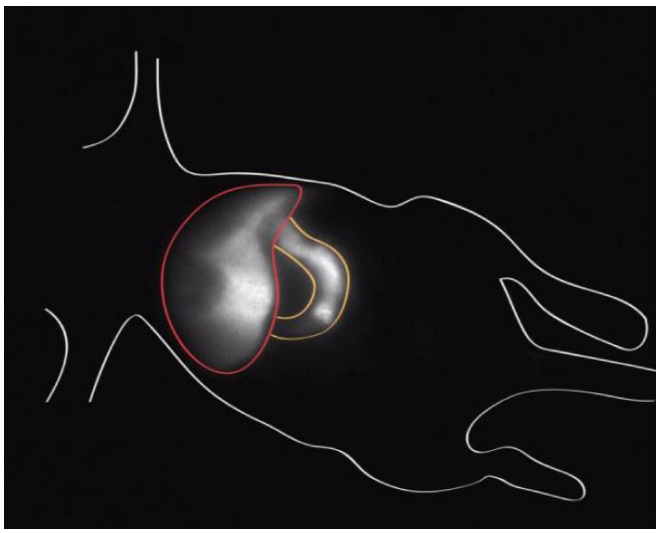

Supplementary Video 2. Hepatobiliary clearance of ICG. The hepatobiliary clearance of ICG is imaged noninvasively at 19.7 fps on an InGaAs camera with a 1200 nm longpass filter.

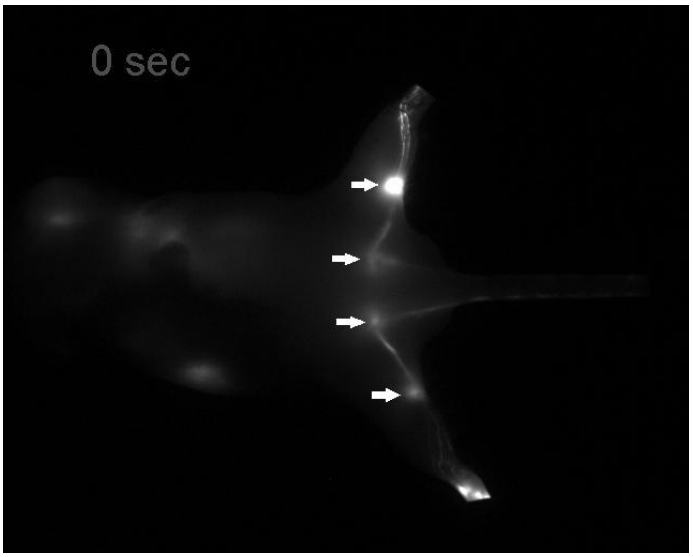

Supplementary Video 3. Real-time SWIR imaging of the lymphatic clearance of ICG. ICG was injected subcutaneously in the footpads and tail of a mouse. The clearance of ICG by the lymphatic system was imaged noninvasively using 50-70 mW/cm^2 of 808 nm excitation light and an InGaAs SWIR camera with 850 nm longpass detection. Each video frame is an average of five frames, each with 50 milliseconds exposure time. Lymph nodes are indicated in the first frame with white arrows.

Supplementary Table 1. The following table details the camera (NIR PIXIS or SWIR NIRvana), the emission filters, and exposure times used for each of the images presented.

Figure		Camera	Filters	Exposure Time (ms)
Figure 1	b (inset)	NIRvana	2x FGL850S, Liquid crystal bandpass filter	10000
Figure 2	d, g	NIRvana	2x FGL1000S, FELH1300	1000
Figure 3	a-1, 2	PIXIS	2x FGL 850S, FELH0850	25
	a-3	NIRvana	2x FGL1000S, FEL1000	500
	a-4	NIRvana	2x FGL1000S, FELH1300	10000
	c, e	PIXIS	FELH0850	5
	d, g	NIRvana	FELH0850, FEL1000, FEL1300	5000
Figure 4	a, b, d, e	NIRvana	FELH1000, FELH1300	100
Figure 5	a, b	NIRvana	FELH0850, FEL1000	500
	c, d	NIRvana	FELH0850, FELH1150	10000
Supplementary Figure 2	a-1	PIXIS	2x FGL850S, FEL1000	500
	a-2	PIXIS	2x FGL 850S, FELH0850	25
	a-3	NIRvana	2x FGL1000S, FEL1000	500
	a-4	NIRvana	2x FGL1000S, FELH1300	10000
	b	PIXIS	FELH0850	20
	c	NIRvana	FELH0850, FEL1000, FEL1300	500
	d-1, e-1	PIXIS	FELH0850	5
	d-2, e-2	NIRvana	FELH0850, FEL1000, FEL1300	5000
	d-3	PIXIS	FELH0850	10
	d-4	NIRvana	FELH0850, FEL1000, FEL1300	5000
Supplementary Figure 3	a-2x	PIXIS	DMLP900, FELH0850	50
	a-6x	PIXIS	DMLP900, FELH0850	100
	c-2x	NIRvana	DMLP900, FELH1300	5000
	c-6x	NIRvana	DMLP900, FELH1300	5000
Supplemental Figure 4	a	NIRvana	FELH1000, FELH1300	100
Supplementary Figure 5	a	NIRvana	FELH0850, FELH1000, FELH1200	50
	b	PIXIS	FELH0850	100
	c	NIRvana	FELH0850, FELH1000, FELH1200	50
	d	NIRvana	FELH0850, FELH1000, FEL1500	500
Supplementary Figure 6	1	PIXIS	2x FGL 850S, FELH0850	10
	2	NIRvana	2x FGL1000S, FELH1000	100
	3	NIRvana	2x FGL1000S, FEL1200	1000
	4	NIRvana	2x FGL1000S, FEL1300	10000
	5	NIRvana	FELH1000, FEL1400	10000
Supplementary Video 1		NIRvana	FELH1000, FELH1300	100
Supplementary Video 2		NIRvana	FELH0850, FELH1000, FELH1200	50
Supplementary Video 3		NIRvana	2x FGL850S, FELH0850	50